Floquet-Engineered Valleytronics in Dirac Systems

Arijit Kundu,* H. A. Fertig, and Babak Seradjeh†
Department of Physics, Indiana University, Bloomington, Indiana 47405, USA
(Received 29 June 2015; published 8 January 2016)

Valley degrees of freedom offer a potential resource for quantum information processing if they can be effectively controlled. We discuss an optical approach to this problem in which intense light breaks electronic symmetries of a two-dimensional Dirac material. The resulting quasienergy structures may then differ for different valleys, so that the Floquet physics of the system can be exploited to produce highly polarized valley currents. This physics can be utilized to realize a valley valve whose behavior is determined optically. We propose a concrete way to achieve such valleytronics in graphene as well as in a simple model of an inversion-symmetry broken Dirac material. We study the effect numerically and demonstrate its robustness against moderate disorder and small deviations in optical parameters.

DOI: 10.1103/PhysRevLett.116.016802

Introduction.—Since the advent of graphene as a two-dimensional electronic material which can be produced in the laboratory [1,2], the possibility of exploiting the valley degree of freedom within it [3] and other Dirac systems has been vigorously studied. An important component of such valleytronic systems is the transport and detection of valley currents. Many of the ideas proposed to do so involve controlling the structure of the system, either using specific edge structures [3] or bulk nanostructures [4,5]. These ideas are limited by the precision they require to control the nanostructure. A particularly interesting way around these limitations combines intrinsic band properties with optics to yield valley-contrasting behavior. In gapped Dirac systems such as MoS_2 and WS_2, or bilayer graphene in a perpendicular electric field, valley currents can be induced using the differing Berry curvatures of the valleys [6–11]. In such systems, circularly polarized light can excite different electron-hole pair populations in different valleys [12–14], leading to a "valley Hall effect" [8,9,15–17].

In this work we discuss a fundamentally different approach to optically controlled valleytronics in the bulk that offers a high degree of tunability in a single sample. In this approach, the light is relatively intense, so that the electronic structure is represented by eigenvalues of a Floquet Hamiltonian. The time dependence of the electric field, rather than intrinsic properties of the material or nanoscale structures, is used to effectively break inversion symmetry and distinguish the valleys. One way to do this, for example in graphene, is by shining an admixture of circularly polarized light of frequencies Ω and 4Ω, which can be coherently generated by the use of nonlinear crystals. As explained below, for appropriate choices of amplitudes and phase offset one can produce a Floquet quasienergy spectrum which is gapped for one valley but gapless for the other. A dc current passed between leads with chemical potentials in this gap is then valley polarized. The degree of polarization can be interrogated with different phase-offsets in the vicinities of each lead, such that the gap closing is in the same or different valleys for each. An example of this behavior for an idealized system is illustrated in Fig. 1. The polarization turns out to be quite robust against disorder and edge effects, as shown below. This system represents an optically controlled valley valve.

This physics can also be applied to systems in which inversion symmetry is already broken, such as graphene on a BN substrate [9] or dichalcogenide materials like MoS_2 and WS_2, which have preexisting gaps that are the same for both valleys. Circularly polarized light may close one gap while opening the other in such materials, again allowing marked preferential conduction for one of the two valleys. Left- and right-circularly polarized light create open channels for opposite valleys, leading to optically controlled valley polarization, as we demonstrate below.

Optically broken inversion symmetry in graphene.—In the presence of a temporally periodic potential, electronic states follow the time-dependent Schrödinger equation. Floquet's theorem [18] guarantees that its solutions as a function of time t have the form $\psi_\alpha(t) = u_\alpha(t)e^{-i\varepsilon_\alpha t}$, with $u_\alpha(t+T) = u_\alpha(t)$, where T is the period of the Hamiltonian $H(t)$, and α includes any quantum numbers required to specify the electronic state. The quasienergies ε_α (which may be restricted to the interval $-\Omega/2 < \varepsilon_\alpha \leq \Omega/2$) are eigenvalues of the "Floquet Hamiltonian" $H_F(t) = H(t) - i\partial_t$, and u_α are the corresponding eigenfunctions.

As a paradigm of these systems we consider the case of graphene, in which the electrons are assumed to hop around on a tight-binding honeycomb lattice [2,19,20], and the effects of the circularly polarized light are implemented via time-dependent phases in the hopping matrix elements [21]. Variations in the intensity and the frequency of the light tune the quasienergy band structure through many distinct topological phases [22]. The energy spectrum includes two valleys of states near the $\mathbf{K}_+$ and $\mathbf{K}_-$ points

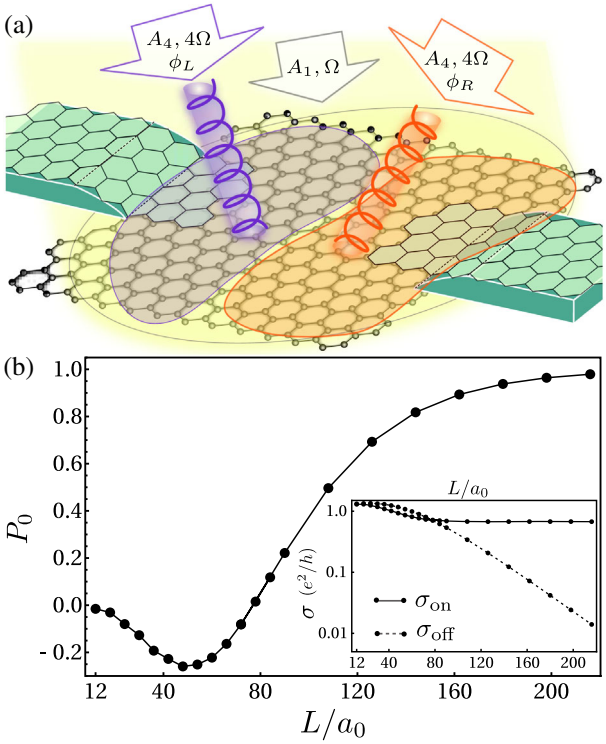

FIG. 1. (a) The schematics of the graphene system: A background laser with frequency Ω and intensity $(c/4\pi)A_1^2\Omega^2$ is supplemented with a circularly polarized fourth harmonic of frequency 4Ω and intensity $(4c/\pi)A_4^2\Omega^2$ with a relative phase offset ϕ_L on the left and ϕ_R right half of the device. (b) The valley polarization $P_0 = 1 - \sigma_{\rm off}/\sigma_{\rm on}$ in a ribbon with periodic boundary conditions vs length L (in units of the lattice constant a_0). The inset shows the on and off conductances, $\sigma_{\rm off}$ and $\sigma_{\rm on}$, respectively. Here, $eA_1a_0/c = 1.0$, $A_4/A_1 = 0.1$, $\Omega/\gamma \approx 1.47$, where $\gamma \approx 2.7$ eV is the hopping parameter, and the ribbon width $w = 6\sqrt{3}a_0$.

of the Brillouin zone, and wave functions are two-component spinors representing the electron amplitudes on the two sublattices of the honeycomb structure. In the presence of a spatially uniform, time-dependent electric field from light normally incident on the graphene plane, the Floquet Hamiltonian in the sublattice basis (u_A, u_B) has the form [22]

$$H_F(\mathbf{k},t) = \begin{pmatrix} -i\partial_t & -\gamma Z(\mathbf{k},t) \\ -\gamma Z^*(\mathbf{k},t) & -i\partial_t \end{pmatrix}, \qquad (1)$$

where $\mathbf{k}$ is the wave vector of the state, γ is a hopping amplitude, $Z(\mathbf{k},t) = \sum_{n=1}^{3} e^{i[\mathbf{k}+(e/c)\mathbf{A}(t)]\cdot\mathbf{a}_n}$, $\mathbf{a}_n$ are the nearest neighbor vectors of a site on the lattice, and $\mathbf{A}(t) = A_1(\cos\Omega t, \sin\Omega t)$ is the vector potential for the electric field, with $\Omega = 2\pi/T$. When $\mathbf{k}$ is set to the $\mathbf{K}_\pm$ point [$\mathbf{K}_\pm = (0, \pm 4\pi/3\sqrt{3}a_0)$, with a_0 the nearest neighbor distance] the lattice symmetry combines with the temporal symmetry so that $Z(\mathbf{K}_\pm, t+T/3) = e^{\mp 2\pi i/3} Z(\mathbf{K}_\pm, t)$, effectively tripling the relevant frequency for the Floquet problem. Because of this, distinct states can cross, rather than repel, at the Floquet zone boundary $\varepsilon_\alpha = \pm\Omega/2$ as A_1 or Ω are varied, leading to topological transitions in the quasienergy band structure.

In this situation such crossings occur at the $\mathbf{K}_\pm$ points simultaneously. This results from a combination of inversion symmetry ($\mathbf{K}_- = -\mathbf{K}_+$) and a form of time reversal symmetry: If $u(\mathbf{K}_+, t)$ is an eigenvector of $H_F(\mathbf{K}_+, t)$, then $\sigma_x u^*(\mathbf{K}_+, -t)$, with σ_x a Pauli matrix, is an eigenvector of $H_F(\mathbf{K}_-, t)$ with the same eigenvalue. Lifting this coincidence of eigenvalues distinguishes the valleys. One way to do this is by changing H_F such that

$$Z(\mathbf{K}_+, -t) \neq Z(\mathbf{K}_-, t), \qquad (2)$$

while retaining the $T/3$ period of $e^{\pm i\Omega t} Z(\mathbf{K}_\pm, t)$ needed for a gap closing, breaking the effective inversion symmetry. In contrast to approaches which use static potentials [4,5], here we seek to use the vector potential to do so, allowing for optical control of the valley-distinguishing properties of the system.

One way this can be done is by adding a fourth harmonic to the vector potential, so that it has the form $A_x + iA_y = A_1 e^{i\Omega t} + A_4 e^{i(4\Omega t+\phi)}$. For this $\mathbf{A}$ the inequality [Eq. (2)] is satisfied, provided $\phi \neq 0, \pi$, while the frequency tripling of $e^{\pm i\Omega t} Z(\mathbf{K}_\pm, t)$ is retained. As illustrated in Fig. 2, gaps at $\mathbf{K}_\pm$ are in general unequal and can be opened and closed around $\varepsilon = \Omega/2$ separately by tuning the optical parameters. Note that the phase offset ϕ may be adjusted by varying the optical path length of the 4Ω light component relative to the Ω component. As we next show numerically, this leads to different band gaps for the two valleys, even allowing the gap to close for one while the other remains open. Thus, the admixture of the two frequencies of light in principle allows one to prohibit a bulk current for one valley while allowing it for the other.

Numerical results.—To test this idea, we have computed the dc conductance at zero temperature for an irradiated graphene strip [22,23]. Armchair graphene ribbons were simulated, with periodic boundary conditions across the width to minimize the edge effects while keeping the size of the system small enough for numerical efficiency. Optical parameters were chosen to produce quasienergy gaps large enough to observe the effect with our simulated system sizes. More realistic optical parameters are discussed below. We also performed simulations for more realistic systems with open boundary conditions. These results are reported below and support our conclusions [24].

The current is introduced from the leads attached to the two ends of the system, while the central graphene region is voltage-biased to align the Floquet zone edge with the average chemical potential of the leads. In this scheme, the entire system is illuminated by light of frequency Ω. Each half of the system around the leads is further illuminated by circularly polarized light of frequency 4Ω with

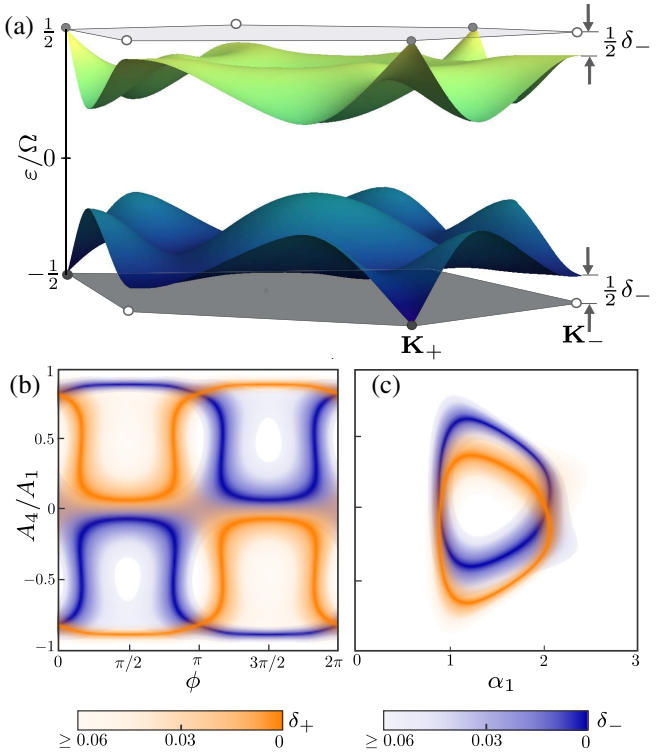

FIG. 2. (a) The bulk quasienergy spectrum in the Brillouin-Floquet zone for uniformly irradiated graphene ($eA_1a_0/c = 1.5$, $A_4/A_1 = 0.6$, $\phi = \pi/2$, $\Omega/\gamma = 1.44$) shows a gap at $\mathbf{K}_-$ and gapless Dirac dispersion at $\mathbf{K}_+$ point. (b) and (c) The quasienergy gaps $\Omega\delta_\pm$ of the $\mathbf{K}_+$ (blue) and $\mathbf{K}_-$ (orange) valleys at $\varepsilon = \Omega/2$ show the gaps may be opened and closed by tuning the optical parameters. In (b) $\alpha_1 \equiv eA_1a_0/c = 1.5$, $\Omega/\gamma = 1$ and in (c) $\phi = 0$, $\Omega/\gamma = 1.44$.

independently controlled values of the phase offset, ϕ_L and ϕ_R. With $\phi_L = \phi_R$, due to the gap for one valley, the system essentially allows only current from the other valley to pass, yielding a valley-polarized current. That this current is valley polarized is confirmed by comparing with the conductance when $\phi_L - \phi_R = (2n+1)\pi$, with n an integer. In this case, the two halves are conductive for opposite valleys so very little net current passes. This means the system behaves as a valley valve [3] which may be opened or closed optically. The relative conductance in these two cases ($\sigma_{\rm on}$ and $\sigma_{\rm off}$, respectively) offer a measure of the valley polarization, $P_0 \equiv 1 - \sigma_{\rm off}/\sigma_{\rm on}$, achieved in the system. The fidelity of the resulting valve can exceed $P_0 = 98\%$, as illustrated in Fig. 1(b) [24]. This is one of our main results.

Effects of edges.—The valley polarization in our proposal results from bulk transport. Because of the existence of multiple Floquet topological phase transitions tuned by frequency [22], the system with open boundary conditions has, in addition, a number of chiral edge states. These edge states can carry current but lack a well-defined valley index. Moreover, they can scatter the bulk states between valleys. Both of these effects can degrade the observed valley polarization, and are particularly noticeable in small systems. We expect that in a sufficiently large sample the degrading effects of the edges will be much reduced.

To support this expectation, we also simulated a more realistic system with open boundary conditions. To minimize edge effects, we employ a geometry in which the leads are connected away from them, as illustrated in Fig. 1(a). This requires relatively large widths, limiting the system lengths one can ultimately study efficiently. Nevertheless, one may still obtain information about the large-length limit by choosing a quasienergy gap that is not too small. We report our results in Fig. 3 and compare them to the case with periodic boundary conditions. The path followed in Fig. 3(a) is chosen so that the gap for one of the valleys vanishes precisely, maximizing the "on" current and thereby the valley polarization. The system with periodic boundary conditions and a gapless $\mathbf{K}_+$ point shows nearly 100% valley polarization for an arbitrary value of the quasienergy gap $\delta_- > 0$ at $\mathbf{K}_-$. For the system with open boundary conditions, a larger gap δ_- is required to have significant valley polarization. Even so, remarkably large valley polarizations are obtained in this case for a relatively small system [24].

Dirac systems with statically broken inversion symmetry.—A second way to break the symmetry of the valley electronic states and realize an optically controlled valleytronic system is by statically lifting the inversion symmetry of the system. Examples of such systems are provided by graphene deposited on boron nitride [28,29] and single-layer MoS_2 [8,30]. A simple description of these

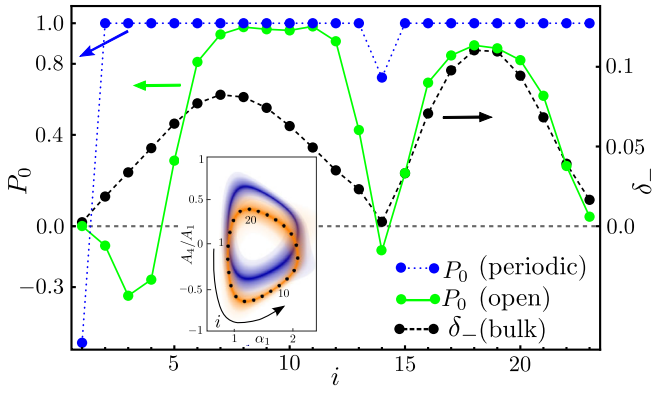

FIG. 3. The valley polarization P_0 for the system with periodic (dotted blue line) and open (solid green line) boundary conditions, respectively. The index i indicates parameter values at points along the $\delta_+ = 0$ (orange) contour shown in the inset, as in Fig. 2(c). The corresponding gap δ_- is also shown (dashed black line). The fixed parameters are as in Fig. 2(a); the chemical potential of the irradiated region is $0.71\gamma \approx \Omega/2$; the periodic system has a full length $L = 2\ell = 288a_0$ and width $w = 6\sqrt{3}a_0$; the open system has $\ell = 27a_0$, $w = 24\sqrt{3}a_0$; the leads have a width $12\sqrt{3}a_0$ and are connected equidistant from the edges across the width and a distance $9a_0$ away from the center.

systems is a tight-binding model on a honeycomb lattice with a staggered potential $\pm\mu_s$ of opposite signs on different sublattices; the low energy electron states at the $\mathbf{K}_\pm$ points are then governed by massive Dirac Hamiltonians. Despite this apparent inversion symmetry breaking, the magnitude of the gap in both valleys is the same and no valley polarization can be realized in equilibrium. Valley polarization in a static region can be achieved in this system via optical absorption [13,31].

In our approach, the gaps at the $\mathbf{K}_\pm$ points can be distinguished by the helicity of the monochromatic circularly polarized light. The Floquet Hamiltonian for the low-energy excitations now takes the form $H_F(\mathbf{k}, t) + M$, where H_F is the same as in Eq. (1), and

$$M = \begin{pmatrix} \mu_s & 0 \\ 0 & -\mu_s \end{pmatrix}. \tag{3}$$

Because of the inversion-symmetry breaking, the quasienergies around the two valleys now evolve differently: for a given helicity, the frequency can be tuned to a value such that there is a gapless $\mathbf{K}_+$ valley crossing $\varepsilon = 0$, and a gapped $\mathbf{K}_-$ valley [24]. Illuminating the two halves of the system with circularly polarized lasers at such a frequency realizes a valley valve. The valve can be turned on and off by switching the helicity of one of the lasers. We have checked that, in this case, the current induced from the leads at energy $E \approx 0$ has a valley polarization exceeding 90%.

Discussion.—To observe the effects we have demonstrated above, energy and length scales in real samples must be chosen appropriately. For example, the temperature in the leads must be less than the quasienergy gap of the gapped valley, namely, $\Omega\delta_-$. This can be tuned optically. For example, at the main frequency $\Omega = 0.2\gamma = 0.54$ eV, a gapless $\mathbf{K}_+$ is obtained at $\alpha_1 = eA_1a_0/c = 0.1$ and laser intensity $I_1 = (1/4\pi c)A_1^2\Omega^2 \sim 10^{14}$ W/m^2. At these values, by varying the ratio A_4/A_1, the gap at $\mathbf{K}_-$ can be tuned to be > 5 meV. Increasing the frequency and the intensity of the laser can produce even larger gaps [24]. Since the conductance of the gapped valley decays over the wave function evanescent length, $\ell_{\rm ev} \propto v/\Omega\delta_-$, the length of the system L must exceed $\ell_{\rm ev}$. Here, v is the Fermi velocity at the valley, which can also be tuned optically. In our estimate, for the aforementioned values, $\ell_{\rm ev} < 500a_0 = 71$ nm.

In practice, there are always extrinsic perturbations limiting the polarization. Prominent among these is disorder, which does so through intervalley scattering. Intuitively, the effect of disorder is to fill in the gap in the quasienergy spectrum. We expect that its effect is controlled by this gap, and that it should not spoil the valley polarization when weak enough. In Fig. 4 we show results of our simulations of disorder-averaged polarizations in the graphene system discussed above [24]. In these simulations we have used random, static on site potentials, with Gaussian distribution of zero mean and standard deviation

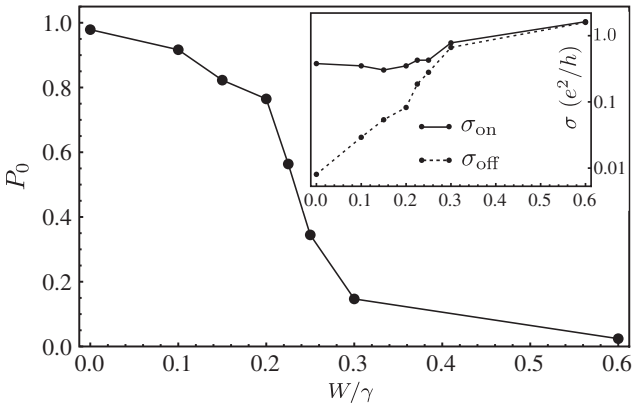

FIG. 4. The polarization of the graphene valley valve vs the strength of on site static disorder potential, W. The parameters are as in Fig. 2(a) and the chemical potential of the irradiated region is $0.71\gamma \approx \Omega/2$. The boundary conditions are open and the dimensions are as for the open system in Fig. 3.

W characterizing the disorder strength. The conductances are each averaged over 25 disorder configurations. Indeed, at larger strengths, disorder causes intervalley scattering and diminishes the valley polarization by increasing $\sigma_{\rm off}$ (see inset). However, when W is sufficiently smaller than the quasienergy gap, here $\Omega\delta_- \approx 0.1\gamma$, the valley polarization we obtain is robust against disorder, exceeding 70% over a significant range of disorder strength. As discussed above, in real samples the quasienergy gap can be tuned to be > 5 meV. Samples with disorder strengths below this appear to be currently available in the lab [32–35]. Thus we believe there is considerable room to vary the parameters of the system without having the effects spoiled by disorder.

Novel forms of electronic states arise as the result of the interaction between electrons and periodic external driving fields. The optically controlled valley polarization and valleytronic devices proposed in this work promise new ways of engineering and utilizing the emergent electronic degrees of freedom in graphene and related Dirac systems.

This work was supported in part by the NSF through Grants No. DMR-1350663, No. DMR-1506263, and No. DMR-1506460, the US-Israel Binational Science Foundation, and by Indiana University. A. K. was supported in part at the Technion by a fellowship of the Israel Council for Higher Education.

*Present address: Physics Department, Technion, 320003 Haifa, Israel.
†babaks@indiana.edu

[1] K. S. Novoselov *et al.*, Science **306**, 666 (2004).
[2] A. H. Castro Neto, F. Guinea, N. M. R. Peres, K. S. Novoselov, and A. K. Geim, Rev. Mod. Phys. **81**, 109 (2009).
[3] A. Rycerz, J. Tworzydlo, and C. Beenakker, Nat. Phys. **3**, 172 (2007).

[4] Y. Song, F. Zhai, and Y. Guo, Appl. Phys. Lett. **103**, 183111 (2013).
[5] M. M. Grujic, M. Z. Tadic, and F. M. Peeters, Phys. Rev. Lett. **113**, 046601 (2014).
[6] W. Yao, D. Xiao, and Q. Niu, Phys. Rev. B **77**, 235406 (2008).
[7] D. Abergel and T. Chakraborty, Appl. Phys. Lett. **95**, 062107 (2009).
[8] K. Mak, K. McGill, J. Park, and P. McEuen, Science **344**, 1489 (2014).
[9] R. Gorbachev *et al.*, Science **346**, 448 (2014).
[10] F. Qi and G. Jin, J. Appl. Phys. **115**, 173701 (2014).
[11] Edbert J. Sie, James W. McIver, Yi-Hsien Lee, Liang Fu, Jing Kong, and Nuh Gedik, Nat. Mater. **14**, 290 (2015).
[12] T. Cao *et al.*, Nat. Commun. **3**, 887 (2012).
[13] H. Zeng, J. Dai, W. Yao, and X. Cui, Nat. Nanotechnol. **7**, 490 (2012).
[14] W. Y. Shan, J. Zhou, and D. Xiao, Phys. Rev. B **91**, 035402 (2015).
[15] Y. D. Lensky, J. Song, P. Samutpraphoot, and L. Levitov, Phys. Rev. Lett. **114**, 256601 (2015).
[16] M. Sui *et al.*, arXiv:1501.04685.
[17] Y. Shimazaki *et al.*, arXiv:1501.04776.
[18] M. Rahzavy, *Quantum Theory of Tunneling* (World Scientific, New Jersey, 2003).
[19] N. Peres, Rev. Mod. Phys. **82**, 2673 (2010).
[20] S. Das Sarma, S. Adam, E. H. Hwang, and E. Rossi, Rev. Mod. Phys. **83**, 407 (2011).
[21] T. Oka and H. Aoki, Phys. Rev. B **79**, 081406(R) (2009).
[22] A. Kundu, H. A. Fertig, and B. Seradjeh, Phys. Rev. Lett. **113**, 236803 (2014).
[23] Z. Gu, H. A. Fertig, D. P. Arovas, and A. Auerbach, Phys. Rev. Lett. **107**, 216601 (2011).
[24] See Supplemental Material at http://link.aps.org/supplemental/10.1103/PhysRevLett.116.016802 for details of realistic optical parameters, numerical methods, Dirac system with broken inversion symmetry, and the length dependence of the valley polarization, which includes Refs. [25–27].
[25] L. Arrachea, Phys. Rev. B **72**, 125349 (2005).
[26] M. P. Lopéz Sancho, J. M. Lopéz Sancho, J. M. L. Sancho, and J. Rubio, J. Phys. F **15**, 851 (1985).
[27] S. Kohler, J. Lehmann, and P. Hänggi, Phys. Rep. **406**, 379 (2005).
[28] B. Hunt, J. D. Sanchez-Yamagishi, A. F. Young, M. Yankowitz, B. J. LeRoy, K. Watanabe, T. Taniguchi, P. Moon, M. Koshino, P. Jarillo-Herrero, and R. C. Ashoori, Science **340**, 1427 (2013).
[29] Zhi-Guo Chen, Zhiwen Shi, Wei Yang, Xiaobo Lu, You Lai, Hugen Yan, Feng Wang, Guangyu Zhang, and Zhiqiang Li, Nat. Commun. **5**, 4461 (2014).
[30] K. F. Mak, C. Lee, J. Hone, J. Shan, and T. F. Heinz, Phys. Rev. Lett. **105**, 136805 (2010).
[31] K. F. Mak, K. He, J. Shan, and T. F. Heinz, Nat. Nanotechnol. **7**, 494 (2012).
[32] X. Du, I. Skachko, A. Barker, and E. Y. Andrei, Nat. Nanotechnol. **3**, 491 (2008).
[33] K. I. Bolotin, K. J. Sikes, J. Hone, H. L. Stormer, and P. Kim, Phys. Rev. Lett. **101**, 096802 (2008).
[34] J. Xue, J. Sanchez-Yamagishi, D. Bulmash, P. Jacquod, A. Deshpande, K. Watanabe, T. Taniguchi, P. Jarillo-Herrero, and B. J. LeRoy, Nat. Mater. **10**, 282 (2011).
[35] D. K. Efetov L. Wang, C. Handschin, K. B. Efetov, J. Shuang, R. Cava, T. Taniguchi, K. Watanabe, J. Hone, C. R. Dean, and P. Kim, arXiv:1505.04812.